LAWRENCE
LIVERMORE
NATIONAL
LABORATORY

LLNL-JRNL-401818

Ultra-fast dynamic compression technique to study kinetics of phase transformations in Bismuth

R. F. Smith, J. O. Kane, J. H. Eggert, M. D. Saculla, A. F. Jankowski, M. Bastea, D. G. Hicks, G. W. Collins

February 29, 2008

Physical Review Letters

Disclaimer

Ultra-fast dynamic compression technique to study kinetics of phase transformations in Bismuth

R.F. Smith, J.O. Kane, J.H. Eggert, M.D. Saculla, A.F. Jankowski, M. Bastea, D.G. Hicks, G.W. Collins

[*]*Lawrence Livermore National Laboratory, P.O. Box 808, CA 94550*

Pre-heated Bi was ramp compressed within 30 ns to a peak stress of ~11 GPa to explore structural phase transformation kinetics under dynamic loading conditions. Under these ultra-fast compression time-scales the equilibrium Bi I-II phase boundary is over-pressurized by $\Delta P \sim 0.8$ GPa. ΔP is observed to increase logarithmically with strain rate, $\dot{\varepsilon}$, above 10^6 s^{-1}. Estimates from a kinetics model predict that the Bi I phase is fully transformed within 3 ns.

PACS numbers: 64.70.Kb, 62.50.1p, 81.30.Hd

Pursuit of a detailed understanding of structural phase-transformation kinetics has been an active area of theoretical and experimental research in condensed-matter physics for several decades [1-13]. Despite this, there remains a lack of quantitative data primarily due to the limitations in experimental techniques to measure these extremely rapid phenomena. Studies of time-dependent transformations have typically used shock-compression, in which a single point in stress-temperature (P_x-T) space is reached over the shock-wave risetime. If P_x lies beyond a phase boundary a two wave profile propagating in the sample can develop due to the equation-of-state (EOS) differences between the two phases. Measurement of the intermediate temporal slope connecting this two-wave structure has been used to infer phase transformation time-scales [5, 6]. Under shock-compression, phase transformation kinetics have also been inferred by spectroscopic [7], x-ray diffraction [8], and recovered micro-structural analysis [9].

Recently-developed ramp-wave-loading (RWL) techniques offer greater sensitivity over shock experiments in detecting phase transformations [10, 11]. Here, we use laser-driven RWL of a 20μm thick pre-heated Bi foil, to sample continuous paths in P_x-T space. The timescale for laser-driven RWL [14] is several to tens of nanoseconds; several times shorter than previously reported phase transition times for Bi I-II [11-13]. By pre-heating the Bi (296 → 476 K) different paths through P_x-T space are explored enabling the mapping out of the Bi I-II phase boundary. Under these rapid compression timescales, the equilibrium Bi I-II phase boundary is determined to be over-pressurized by $\Delta P \sim 0.3 \rightarrow 0.8$ GPa. The onset of significant over-pressurization occurs at a strain rate, $\dot{\varepsilon}$, of 10^6 s^{-1}. For higher $\dot{\varepsilon}$, ΔP increases logarithmically. A non-equilibrium model for interfacial velocity coupled to a multi-phase EOS predicts that the full transformation

time from the ambient Bi I phase is ~3ns. The experiments reported here are, to our knowledge, the first time multiple-wave features associated with phase-transformations have been observed under laser-driven compression.

The laser-driven RWL target design consists of a 125μm polyimide [$C_{22}H_{10}N_2O_5$] foil, a 325-400μm vacuum gap and the Bi/window target (Fig. 1). One beam of the Janus laser at 527 nm delivered 150-200J in a 4ns square pulse onto the polyimide which generated an ablatively-driven shock. A kinoform phase plate inserted into the Janus beam-line, produced a ~1 mm square, planar ($\Delta I/I$ ~ 5%) region at the focal plane. After shock-breakout from the rear surface, the polyimide rarefies across the vacuum gap, monotonically loads-up against the Bi sample, and launches a ramp-compression wave. The Bi was coated directly onto either a LiF or sapphire window via e-beam deposition under conditions which yielded a ~5 μm long tapered-crystallite structure in the stress loading direction and a ~1 μm in-plane grain size [15]. The Bi rhombohedral crystal structure was orientated along the c-axis [001] in the growth direction with random orientation in-plane and was measured to be fully dense (9.78 g/cc) to within an accuracy of 0.6%. The ultra-pure LiF and sapphire crystals had [100] and [001] axial orientations, respectively. The time history of the transmitted compression wave was recorded by measuring the Bi/window interface velocity, $u(t)$, with a line-imaging velocity interferometer (VISAR) with a velocity accuracy of ~10 m/s and a streak camera temporal resolution of ~0.1ns [16]. The refractive index change with density within the LiF and sapphire windows has a constant correction as a function of P_x, which in our analysis, we assume to be independent of temperature in the 293 → 532K range [11].

The loading history, $P_x(t)$, was estimated by replacing the Bi/window target with an Al/LiF target. By measuring $u(t)$ at the impedance-matched Al/LiF interface and integrating the equations of motion backwards in space using the equation-of-state of aluminum, $P_x(t)$ can be estimated for any laser irradiation-target configuration [17]. The ramp-compression wave shown in Fig. 1 with a 325μm vacuum gap and 150J laser energy has a peak P_x of ~11 GPa and a rise-time of ~30ns. The ramp rise-times (15-35ns) and peak P_x (8-11 Gpa) are a function of vacuum gap size and laser energy.

The initial Bi temperature, T_i, was controlled, by resistive heating, to an accuracy of ± 5K to explore different regions of P_x-T space. The output from the line imaging VISAR, $u(x, t)$, is shown in Fig. 1 for a Bi/sapphire sample, with T_i = 463K. Shown in Fig. 2 are recorded Bi/LiF and Bi/sapphire interface velocity histories for T_i spanning 296 - 532K. All velocity profiles are characterized by a smooth ramp with a shoulder followed by a plateau and a fast rise. The shoulder-point velocity, u_{sp}, falls with increasing T_i.

The transformation from the smoothly rising load profile in Fig. 1 to the structured transmitted wave profiles in Fig. 2 is understood by considering the target dynamics in Lagrangian co-ordinates (Fig. 3). $P_x(t)$ may be represented by a characteristic (x-t trajectories) propagating through the Bi sample with a slope inversely proportional to the Lagrangian sound speed, $C_L = \frac{\rho}{\rho_0}\left(\frac{\partial P_x}{\partial \rho}\right)^{\frac{1}{2}}$. When $P_x(t)$ coincides with the equivalent hydrostatic pressure, P, associated with the Bi I-II phase boundary the material enters a mixed phase region. The resultant drop in C_L causes a separation of characteristics and a shoulder point followed by the plateau on the recorded Bi/LiF interface velocity, $u(t)$. In our analysis we use u_{sp} as a signature of the onset of higher phases (> Bi I). The observed

drop in u_{sp} with T_i is related to the negative P-T slope of the Bi I-II phase boundary. When the rate of compression is comparable to the time-scale for phase transformation lattice re-ordering, an evolving mixed phase region exists over a range of P_x resulting in a 'ramped' plateau. Once fully transformed from Bi I into a higher phase, C_L increases generating a shock and a fast *u(t)* rise. For the sapphire window targets, impedance matching at the Bi/sapphire interface increases the interface stress. Thus, the phase transition in Bi will originate both at the drive surface and at the Bi/sapphire interface. It is the transition at the Bi/sapphire interface that we observe in our wave profiles. The value of u_{sp} are markedly different for the LiF and sapphire windows (~3x, see Fig. 2). Only by extracting the stress at the phase transition in the Bi by impedance matching do we obtain consistency between the data for the two window materials, as discussed below.

u_{sp} is related to an equivalent particle velocity within the bulk Bi sample by using an analytic Bi I EOS [18] with a perfectly-elastic to perfectly-plastic transition determined by our data, and assuming an elastic EOS for both Sapphire (P_x=44.2u_p +4.7 u_p^2 [19]) and LiF (P_x=17.35 u_p +6.23 u_p^2 [20]) [P_x (GPa), u_p (km/s)]. Due to impedance matching between Bi and the LiF window, incoming stress waves are reduced upon reflection back towards the drive surface. Thus, the plateau observed for the phase transition corresponds to a stress originating at the drive surface. The impedance matching is performed by solving for the P_x-u_p corresponding to a forward-going ramp in the LiF window and a forward and backward-going ramp in the bismuth. The intersection of backward- and forward-going ramps in the Bi gives the bulk-Bi u_p. The samples are sufficiently thick that the reflected waves from the Bi/LiF interface do not reach the initial loading surface

until late times. For the Bi/sapphire samples, the plateau we observe is associated with the transition originating at the Bi-Sapphire interface, so no impedance matching is required and the stress is given directly by the sapphire P_x-u_p relation. That our interpretation of the origin of the plateaus and the impedance-matching procedures are correct can be ascertained by the consistency of the LiF and Sapphire window transition pressures shown in Fig. 4.

Since these experiments are uniaxially loaded $P_x(u_{sp})$ needs to be related to hydrostatic pressure, P, in order to draw comparison against equilibrium phase boundaries. In the analysis of Fowles [21] using the Le´vy–von Mises yield criterion [22] the stress deviation between P_x and P corresponds to two-thirds the yield strength, Y. For an elastic-plastic material, $Y = (1\text{-}2\nu)/(1\text{-}\nu)*P_{x(E\text{-}P)}$ [21]. Here, $P_{x(E\text{-}P)}$ is the elastic-plastic (E-P) transition stress and Poisson's ratio, ν, is assumed constant at 0.34 over the temperature range studied [23]. The average $u_{E\text{-}P}$ for the Bi/LiF and Bi/Sapphire targets are 0.031 ± 0.006 km/s and 0.015 ± 0.003 km/s, respectively, and are observed to be approximately constant across the initial temperature range sampled (Fig. 2). Using the Bi I EOS [18], $u_{E\text{-}P}$ is equivalent to a bulk Bi stress, $P_{x(E\text{-}P)}$ of 0.55 ± 0.09 GPa and Y of 0.28 ± 0.04 GPa. This is ~3 times higher than has been previously reported on shock experiments [12]. The insensitivity of Y to temperature suggests no thermal softening of the pre-heated Bi sample. This is in contrast to the reported eight-fold decrease in the yield strength of Bi when heated close to melt and stressed over tens of seconds time-scales [24].

To estimate the temperature of the phase transformation, T, an isentrope $T(P)$ is constructed through T_i using a Bi I EOS [18]. This technique of converting the u_{sp} to a

point in *P-T* space does not require *a priori* knowledge of $P_x(t)$ at the loading surface or an exact knowledge of the target thickness. The inferred *P-T* points are shown in Fig. 4 alongside the Bi I, II and liquid equilibrium phase boundaries [25]. The error bars in *P* reflect the uncertainty in measuring the u_{sp}.

The ability to control T_i in the 293-440 K range enables the Bi I-II phase boundary to be mapped out. Under the ultra-fast timescales reported here, the inferred *P-T* points lie above the Bi I-II equilibrium phase boundary by ~0.3→0.8 GPa. The extent of over-pressurization, ΔP, within the data reported here and those inferred from the shock compression data of Asay [12] and the ramp compression data of Bastea [11] is related to the strain rate [26], $\dot{\varepsilon}$, over which the equilibrium phase boundary is traversed, see Fig 5. Here, $\Delta P = P - P_{\text{I-II Equilibrium}}$ along the isentrope. The errors in ΔP come directly from the uncertainty in P (Fig. 4). The Bi I-II equilibrium boundary is assumed to be correct [18]. We observe a threshold value for $\dot{\varepsilon}$ of ~1.4x10^6 s^{-1} above which ΔP scales logarithmically. A fit to the data shows, $\Delta P = 0.655 \log\left(\dot{\varepsilon} / \dot{\varepsilon}_o\right)$ for $\dot{\varepsilon} > \dot{\varepsilon}_o$, where $\dot{\varepsilon}_o = 1.4\text{x}10^6$ s^{-1}. In recent diamond-anvil-cell (DAC) experiments ($\dot{\varepsilon}$ ~ 10^{-6} s^{-1}), ΔP of 0.032 GPa is reported [13]. This scaling of ΔP with $\dot{\varepsilon}$ reported here for the Bi I-II transformation is similar to the time dependence of ΔP reported for Ti and Y for $\dot{\varepsilon}$ ~9 orders of magnitude slower [27].

For trajectories above the Bi I-II-Liquid triple point (T_i > 440K, shown as open circles in Fig. 5), ΔP is estimated from the difference between the measured value of P and the

assumed linear meta-stable extension of the Bi I-II equilibrium boundary. Additional uncertainty associated with these points is related assumption of a slow melt. However, no multi-wave features at pressures associated with the melt line are observed in our data which suggests that for the $\dot{\varepsilon}$ reported here melting does not occur.

The loading path through *P-T* space is related to the competing timescales of compression and transformation kinetics. If the phase transformation timescales are short relative to the ramp compression time the *P-T* associated with the phase change will agree well with the equilibrium phase boundary. To estimate the transformation time-scales, the wave propagation in the Bi/window samples are modeled using the Andrews-Hayes method [5, 28] coupled to a multiphase EOS to advance material elements in (P_x, T, **z**), space where the components of the vector **z** are the mass fractions of the individual phases. A detailed discussion of the non-equilibrium modeling as well as the input parameters to the simulation may be found in ref [25]. This dynamic model qualitatively reproduces the observed VISAR record (Fig. 2), including the sloped 'plateau' and the subsequent fast rise. The model requires as an input knowledge of the temporal history of the compression wave and the thickness of the target material. The same time constants (fitting parameters) were used in the model for both the Bi/LiF and Bi/Sapphire targets. The calculated full transformation time, τ, from the Bi I phase, when compressed initially along the room temperature isentrope, is ~3ns. Applying the same kinetics model to fit the Bi profiles measured by Bastea *et al*. [11] suggests a $\tau \sim 60$ns. In those experiments a 0.3-0.5mm thick Bi sample attached to a LiF window was compressed to 15 GPa over 300ns.

We have demonstrated a laser-driven dynamic compression technique at high compression rates to study time-dependent effects on phase transformations in Bi. Pre-heating the Bi sample enabled the mapping out of the Bi I-II phase boundary. At these ultra-fast loading rates we observe the largest reported over-pressurization of the Bi I-II phase boundary ($\Delta P \sim 0.8$ GPa). ΔP is shown to have a dependence on the strain rate, $\dot{\varepsilon}$, through the equilibrium phase boundary. Non-equilibrium modeling coupled to a multi-phase Bi EOS is shown to give good qualitative agreement to the data and predicts that under ramp compression over ~10ns, full transformation from the Bi I phase occurs after 3ns. The ramp rise-times reported here are ~10 times faster than previously reported in RWL experiments. Laser-driven RWL represents a new experimental technique for studying phase transformation kinetics.

* This work performed under the auspices of the U.S. Department of Energy by Lawrence Livermore National Laboratory under Contract DE-AC52-07NA27344.

References

[1] A.N. Kolmogorov, Bull. Acad. Sci. U.S.S.R., Phys. Ser. **3**, 555 (1937); W.A.. Johnson, R.F. Mehl, Trans. Am. Inst. Min. Metall. Pet. Eng. **135**, 416 (1939); M. Avrami, J. Chem. Phys. **7**, 1103 (1939).

[2] G. E. Duvall and R. A. Graham, Rev. Mod. Phys. **49,** 523 (1977).

[3] A.C. Pan *et al.*, J. Phys. Chem. B **110**, 3692 (2006).

[4] H.A. Schöpe *et al.*, Phys. Rev. Letts **96**, 175701 (2006).

[5] D.B. Hayes, J Appl. Phys. **46**, 3438–3443 (1975).

[6] J.C. Boettger, and D.C. Wallace, Phys. Rev. B **55**, 2840, (1997).

[7] M.D. Knudson and Y.M. Gupta, J. Appl. Phys. **91**, 9561 (2002).

[8] D.H. Kalantar *et al.*, PRL **95,** 075502 (2005).

[9] T. Sano *et al.*, Appl. Phys. Lett. **83**, 3498 (2003).

[10] D.H. Dolan *et al.*, Nat. Phys., 3, 339 (2007); M. Bastea *et al.*, Phys Rev B **75**, 172104 (2007).

[11] See M. Bastea *et al.*, Phys. Rev. B, **71**, 180101(R), (2005) and references within.

[12] J.R. Asay, J. Appl. Phys. 45, 4441 (1974); J.R. Asay, J. Appl. Phys. **48**, 2832-2844 (1977).

[13] I.C. Getting, Metrologia **35**, 119-132 (1998).

[14] R.F. Smith *et al.*, Phys. Rev. Letts **98**, 065701 (2006).

[15] A.F. Jankowski *et al.*, Mat. Sci. Eng. A **431**, 106-108 (2006).

[16] P.M. Celliers *et al.*, Rev. Sci. Instrum. **75**, 4916 (2004).

[17] See R.F. Smith *et al.*, Phys. Plas. **14**, 057105 (2007) and references within.

[18] J.N. Johnson *et al.*, J. Phys. Chem. Solids **35**, 501 (1974).

[19] O.V. Fat'yanov, R.L. Webb and Y.M. Gupta, J. Appl. Phys. 97, 123539 (2005).

[20] Y.M. Gupta, G.E. Duvall, G.R. Fowles, J. Appl. Phys. 46, 532 (1975).

[21] G.R. Fowles, J. Appl. Phys. **32**, 1475 (1961).

[22] R. Hill, *The Mathematical Theory of Plasticity* (Oxford University Press, New York, 1950).

[23] I.J. Fritz, J. Appl. Phys. **45,** 60 (1974).

[24] V.A. Skudnov *et al.*, Metallovedenie I Termicheskaya Obrabotka Metalov, No. 12, 54 (1969).

[25] J.O. Kane, R.F. Smith, AIP Conf. Proc. **845**, 244 (2006).

[26] The strain rate, $\dot{\varepsilon} \equiv [d(u)/d(t)]/[C_L(u)]$, where u is the measured particle velocity and C_L is the Lagrangian sound speed calculated here from a tabulated Bi I EOS.

[27] A.K. Singh *et al.*, J. Appl. Phys. 53, 1221 (1982); A.K. Singh *et al.*, Bull. Mater. Sci. 5, 219 (1983).

[28] D.J. Andrews, J. Comp. Phys. **7**, 310–326 (1971).

Figures

Fig. 1 – Ramp-compression wave applied to Bi target for target and irradiation conditions shown in the insert. The output of the line VISAR is shown for an initial Bi/Sapphire for T_i of 463K. One fringe shift is equivalent to a Bi/LiF interface velocity of 0.257 km^{-1} s^{-1}.

Fig. 2 - (a) The time histories of the Bi/LiF interface velocity with T_i (A → F) of 296, 349, 443, 467, 493 and 495K, respectively. (b) The time histories of the Bi/Sapphire interface velocity with initial target temperatures (a → f) of 296, 343, 393, 443, 463, and 476, respectively. The 463K (e) profile was extracted from the VISAR data shown in Fig. 1. Trace *a* was taken as with a faster loading ramp wave which result in a faster rise-time towards the shoulder point and a shorter plateau. Trace *b* was a 50 μm thick sample as opposed to the standard 20μm thick samples. Also shown are velocity profiles calculated with a non-equilibrium model using the input pressure profile from Fig. 1.

Fig. 3 - A characteristics view of wave propagation through a Bi/LiF sample.

Fig. 4 – *P-T* plot of Bi shown with I, II and Liquid equilibrium phase boundaries. Points from a series of pre-heated Bi samples are shown for the two different window materials used (LiF, Sapphire). Trajectories through phase space along the isentrope and from non-equilibrium modeling with T_i of 393K deviate from each other at the Bi I-II phase boundary.

Fig. 5 – Over-pressurization, ΔP, as a function of strain rate, $\dot{\varepsilon}$, through the equilibrium phase boundary.

Smith *et al.* – Fig. 1

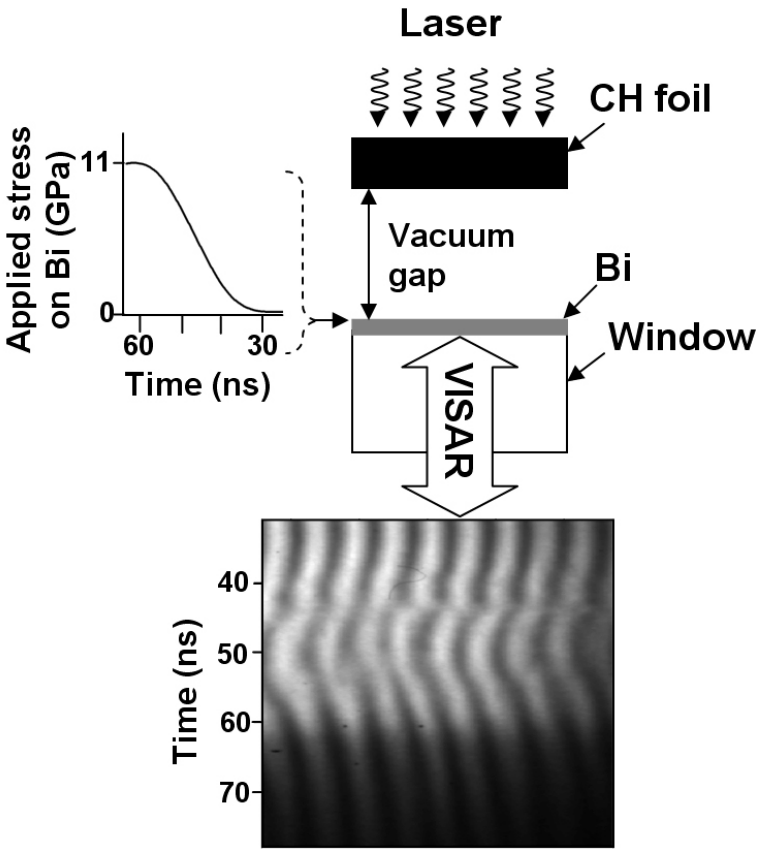

Smith *et al.* – Fig. 2

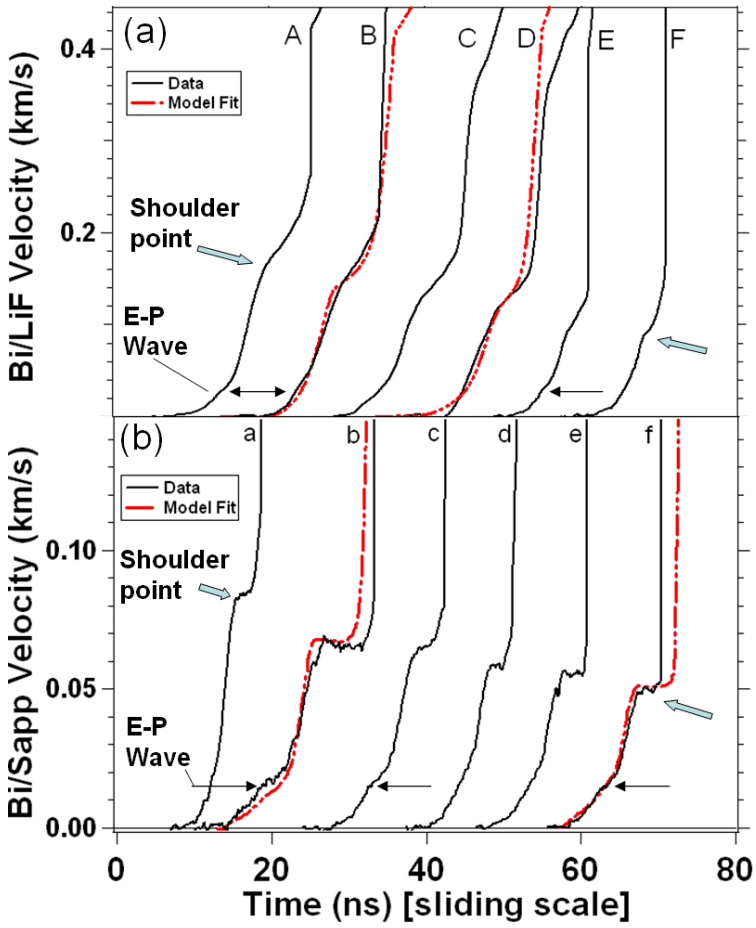

Smith *et al.* – Fig. 3

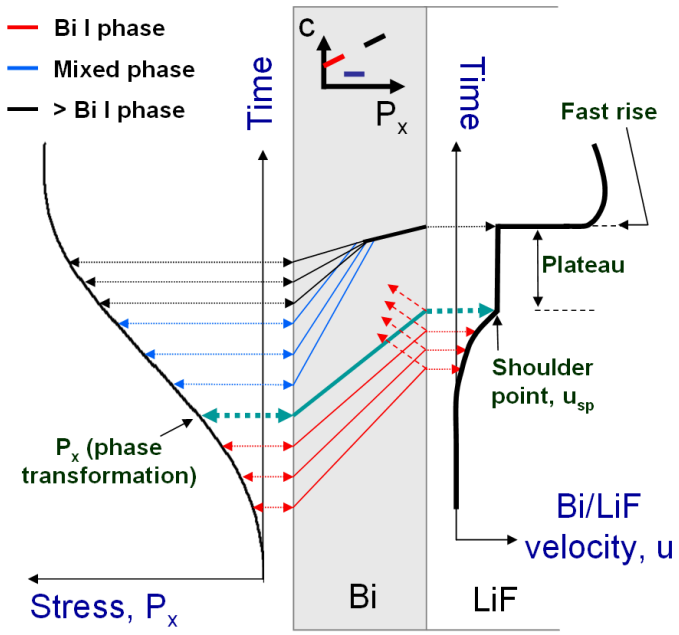

Smith *et al.* – Fig. 4

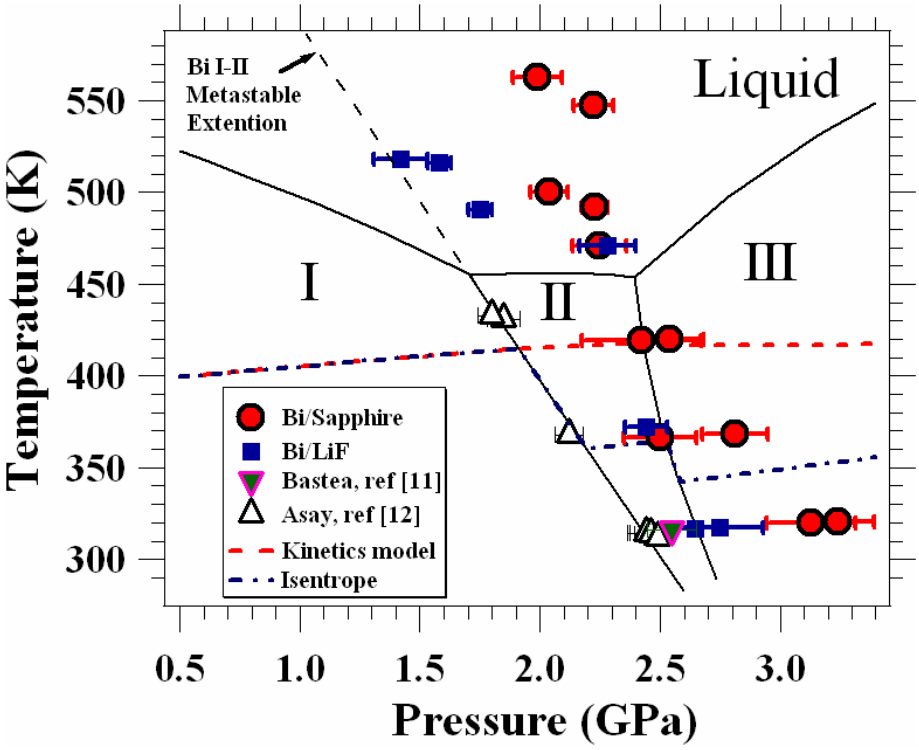

Smith *et al.* – Fig.5